International Symposium
On Turbulence and Shear Flow
Phenomena (TSFP-9)
June 30 - July 3, 2015 *Melbourne, Australia*

'SHAKE THE BOX': LAGRANGIAN PARTICLE TRACKING IN DENSELY SEEDED FLOWS AT HIGH SPATIAL RESOLUTION

Daniel Schanz, Andreas Schröder and Sebastian Gesemann
Department of Experimental Methods
Institute of Aerodynamics and Flow Technology
German Aerospace Centre (DLR)
Bunsenstr. 10, 37073 Göttingen
Email: daniel.schanz@dlr.de; andreas.schroeder@dlr.de

Bernhard Wieneke
LaVision GmbH
Anna-Vandenhoeck-Ring 19, 37081 Göttingen
Email: bwieneke@lavision.de

ABSTRACT

Great progress has been made in the field of optical and particle based measurement techniques for (turbulent) flow investigations in the past few decades. The rise of digital high- frame rate and dual-frame cameras and powerful pulse lasers enabled a special breakthrough for PIV and PTV measurement techniques. PIV delivers spatially well resolved velocity vectors in a 2D- or 3D-domain in an Eulerian frame of reference and thus the velocity gradient tensor, while PTV determines Lagrangian particle tracks with a limited spatial density, but high accuracy of the particle velocity estimation due to temporal filtering by appropriate (polynomial) fitting functions. Therefore, from properly designed 3D PTV experiments high-resolution turbulence statistics can be calculated including e.g. mean profiles or the Reynolds stress tensor.

The newly developed 4D PTV technique *Shake The Box* (STB) has been introduced recently (Schanz et al. 2013b, Schanz et al. 2014) and is capable of delivering highly accurate *and* dense velocity information in a volume of the flow by reconstructing a large amount of Lagrangian particle tracks from a time series of particle images. The main advantages of such data for turbulence (shear) flow research are the possibility to bridge between Eulerian and Lagrangian frames of reference and to provide relevant measures for local and global velocity statistics at high spatial and temporal resolution.

INTRODUCTION

Since almost ten years tomographic PIV methods (Elsinga 2006), in snapshot or time-resolved mode, have been developed and applied to various (turbulent) flow regimes (Scarano 2013) in order to determine instantaneous 3D velocity vector volumes from particle images of relatively densely seeded flows (~0.05 ppp (particles per pixel)). However, for all PIV based approaches the spatial resolution of the local instantaneous velocity measurement is limited by the finite size of the cross-correlation window, which acts as a low-pass filter biasing the measurement particularly in presence of strong velocity gradients. Two further basic limitations of PIV can be described by the dynamic velocity range (DVR) which is typically in the order of 1:100 and the dynamic spatial range (DSR), which is basically limited by the resolution of the used camera sensor (Adrian 1997). Several methods have been developed in order to overcome these limitations; nevertheless, only particle-tracking approaches have been found capable of delivering reliable results for at least the mean flow statistics near interfaces and walls (Kähler et al. 2012) or in strong-shear flow.

On the other hand 3D PTV algorithms have been mature since more than 20 years calculating Lagrangian tracks and subsequent statistics based on particle images of relatively sparsely seeded flows (< 0.01 ppp) at high temporal resolution (Maas et al. 1993; Malik et al. 1993). Both 'conventional' 3D- evaluation methods reconstruct the three-dimensional particle positions relying on an individual treatment of every single snapshot and a *subsequent* treatment of the results for consecutive images (volume correlation for tomo PIV (Elsinga 2006), advanced particle partner matching for 3D PTV (Ouellette et al. 2006)).

In contrast the newly developed 4D PTV technique STB seizes the temporal information in subsequent particle images directly for a highly accurate and ghostless Lagrangian track reconstruction of densely seeded flows (around 0.1 ppp) using a prediction and iterative matching ('shaking') scheme, while the hardware and measurement requirements are the same as for time-resolved tomo PIV or 3D PTV systems.

Nevertheless, with common camera and laser techniques time-resolution of all flow features captured in long time-series of images from several viewing directions is simply not possible for most of the aerodynamically relevant flows at high Reynolds numbers. For such flows at high speed velocities a new measurement technique is

under development at DLR using a (four to eight) multi-pulse 3D PTV technique which adapts the STB evaluation scheme based on a few subsequent particle images gained by volumetric illumination with four or more laser light pulses with two perpendicular states of polarization and respective cameras equipped with polarizing filters (see Schröder et al. 2013).

SCHEME OF THE STB- METHOD

Tomo PIV is well known for delivering Eulerian velocity data on a regular 3D grid in a robust way and thus the full (time-dependent) velocity gradient tensor with a relatively high spatial resolution (corresponding to the correlation window/volume size), but with relatively high computational costs, low accuracy (>0.15 px) and inherent bias errors due to ghost particles. Temporally oversampled 3D PTV methods deliver accurate Lagrangian tracks, enabling even the derivation of accelerations, but with a very limited spatial resolution for each time step. The STB technique is able to overcome the restrictions in tomo PIV and classical PTV methods by using the temporal information directly in the reconstruction process.

The 4D-PTV technique, *Shake The Box* (STB), was introduced in 2013 and at the time applied to an experimental dataset (see result of a tomo PIV evaluation by Davis 8 in figure 2), showing profound advantages over conventionally used techniques to evaluate time-resolved three-dimensional data (tomographic PIV, 3D PTV) (Schanz 2013b). For the work presented here, the method is characterized in terms of accuracy, completeness of the reconstruction, occurrence of ghost particles and computation time by means of synthetic data.

The STB algorithm is based on recent developments for increasing the accuracy of 3D- calibration and -particle positioning (mainly in the frame of (hybrid) tomo PIV/PTV approaches) namely the iterative particle reconstruction (IPR) method (Wieneke 2013), the high sub-pixel accuracies for all lines-of-sight using volume self-calibration (Wieneke 2007) and the determination of the local optical transfer functions (OTF) of particles (Schanz et al. 2013a). Additionally, the innovative 4D character of the STB algorithm is relying on the condition that real particles within a volume cannot disappear between time steps. After an initialization process based on IPR or a tomographic SMART reconstruction - identifying several thousand particle tracks of a certain length and intensity in the first few image samples (which already dramatically reduces the number of ghosts) - a growing and further saturating number of particles can be predicted along all found tracks for time t = n +1. The predicted positions exhibit already a sufficient accuracy for a next round of the particle image matching resp. 'shaking' scheme which can cover even large accelerations of the particle due to the given sparsity of the true particle distribution in 3D space and the ongoing identification of particles in tracks during the STB reconstruction. After a few successive time steps the ambiguity of the ill-posed reconstruction problem present for each *single* time step is nearly diminishing in this 4D approach even for high seeding densities. Further on, only those particles which are newly entering the volume have to be triangulated for some time steps before being tackled by the same scheme. In a second step the reconstruction process of the STB is going backwards in time using all found tracks of the first forward iteration in order to enhance the accuracy, connect ending tracks and fill up the temporal domain of the initialization process. For difficult reconstruction problems a third and a fourth pass can be applied in forward and backward direction in time in order to find residual tracks and their connections. The final results of the STB algorithm are highly accurate, spatially dense and long Lagrangian tracks within the reconstructed measurement volume.

Under the assumption that the trajectories of nearly all particles within the system are known for a certain number of time-steps, the STB- evaluation scheme for a single time-step is as follows:

1. Fit a function (polynomial) to the last n positions of every tracked particle,
2. Predict the position of the particle in the next time-step n+1 by evaluating the fitted polynomial,
3. Shake the particles to their correct position and intensity, eliminating the error introduced by the prediction,
4. Find new particles entering the measurement zone using triangulation on the residual images,
5. Shake all particles again to correct for residual errors,
6. Iterate steps 4 and 5, if necessary,
7. Add new tracks for all new particles that are identified within four consecutive time-steps,
8. Remove particles from track system either if leaving the volume or if intensity falls below threshold.

The process of 'shaking' the particles was first described by Wieneke in the scope of the technique of 'Iterative reconstruction of Volumetric Particle Distribution' (IPR) (Wieneke 2013). It compares iteratively the reprojected particle image weighted with the calibrated OTF with the original image in several shaking steps in order to find a 3D position which minimizes the residual image for all camera projections for reaching high position accuracies. Using the described scheme, the STB algorithm is capable of working through long time-series, extending known tracks step-by-step and continually adding particles that enter the measurement zone to the list of tracked particles. As the major part of the system is already solved after the prediction, only small errors need to be corrected by shaking and by adding new particles. Therefore, the method is computationally very effective.

Especially for deep volumes the data size needed for a STB evaluation delivering only a list of x-y-z-particle positions, related track-id and velocity distributions is much smaller than a respective voxel representation of a tomo PIV evaluation step. As one consequence the computing time for a STB reconstruction of a present implementation is about 3 to 20 times faster than the fastest actual tomo PIV algorithm (the latter value for lower particle numbers) and is mainly depending on the number of particles within the measurement volume. Therefore, STB is predesignated for effectively reconstructing dense particle trajectories in flows with a large and deep measurement volume.

BENCHMARK OF STB-METHOD USING SYNTHETIC DATA

In order to quantitatively capture and compare the accuracy of different methods, a process to extract synthetic tracks from a known vector field was designed (Schanz et al. 2014). Systems of synthetic tracks were derived from divergence-free source vector fields taken from a tomographic PIV experiment. Time-series of 50 snapshots each were created for different seeding densities ranging from 0.01 ppp to 0.125 ppp and projected onto four virtual cameras using parallel projection.

In order to compare the results of the STB method (see figure 1) to the technique commonly used for processing high-density three-dimensional data, tomographic reconstructions of the synthetic images were performed, using an DLR implementation of the MLOS-SMART algorithm (Atkinson et al. 2009). As this technique does not utilize temporal information, only five volumes enabling a direct comparison to STB data in converged state per seeding density were reconstructed. In order to be able to compare position accuracy as well as the fraction of undetected and ghost particles, a 3D Gaussian peak finder from LaVision Davis 8 was used to identify particle positions within the reconstructed volume.

Comparing the results gained by STB with standard tomo PIV, it becomes obvious that the inclusion of the temporal information opens a door to achieve results of much higher quality. The number of correctly identified particles remains above 99.5 %, even for 0.125 ppp. The ghost particle problem is nearly completely resolved – for 0.125 ppp a ghost particle proportion of 0.033 % is determined. In particle numbers, this means that 36 ghost particles occurred for STB, while MLOS-SMART produced over 280,000. For lower seeding densities ghost levels of less than 0.02 % down to zero can be reached. The (nearly) absolute prevention of ghost particles, combined with the highly accurate image matching (shaking) process leads to a significant increase in achievable accuracy: For low seeding densities (≤ 0.05 ppp), errors below 0.0008 px are found – a factor of over 200, compared to tomographic reconstructions. The error rises for higher seeding densities, but still remains below 0.02 px even for 0.125 ppp, which is more than an order of magnitude lower compared to SMART (0.31 px) and a factor of six lower compared to SMART at 0.01 ppp (0.13 px). An overview of the comparison of all values determined in this study is given in table 1. The data in the table show better results than given in the accuracy estimation from Schanz et al. in 2014 due to some new developments and fine-tuning steps, which are advantageous for both experimental and synthetic particle images. Especially the higher position accuracy can be essentially ascribed to the newly implemented iterative reduction of shaking step sizes down to a small fraction of a pixel, which results in such very high accuracies solely for synthetic images.

Nevertheless, for realistic experimental scenarios or synthetic images plus noise the superiority of the STB particle position accuracies to the ones of a tomo PIV approach is slightly reduced, while the very low ghost-level of the STB technique remains nearly constant as a big advantage (Schanz et al. 2014).

A subsequent temporal fit of the found trajectories can additionally improve particle position accuracy and enables the derivation of Lagrangian velocities and accelerations. The STB-method allows for the first time to extract highly accurate Lagrangian information from densely seeded flows. Such information is especially valuable for the validation and development of CFD codes and turbulence models, demanding precise measurements of derivation tensors. Turbulence research benefits greatly from the availability of accurate velocity and acceleration measures e. g. for Lagrangian PDFs and two-point-correlations of Eulerian and Lagrangian measures.

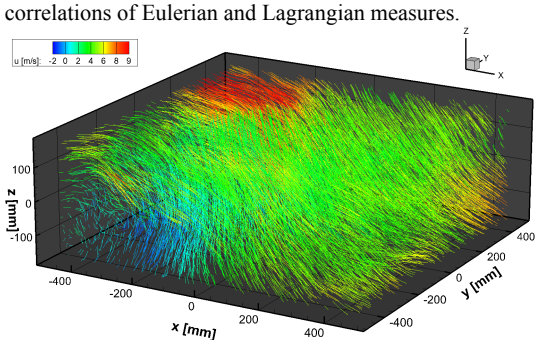

Figure 1: Source tracks from synthetic data created for ppp = 0.01. Only 15 time-steps are shown. Flow in positive x-direction, color coded stream-wise velocity.

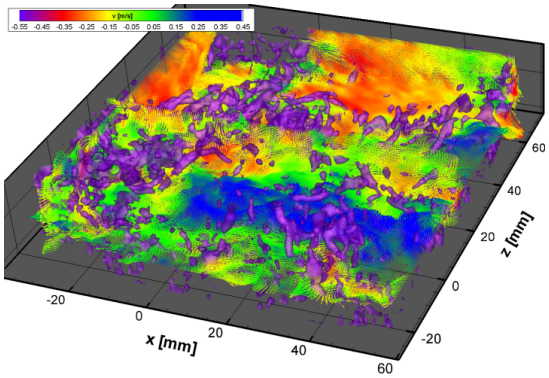

Figure 2: Iso-surfaces of constant λ_2 revealing vortical structures in the instantaneous velocity distribution in a turbulent "periodic hill" flow at TU Munich water tunnel based on a classical tomo PIV evaluation.

During the *4th international PIV Challenge* in spring 2014 the STB technique (at the respective development stage) has been applied to both synthetic 3D test cases; to the predesignated time-resolved case D (see one time step with ~200,000 particles in Figure 3) and with a hybrid tomo PIV and STB approach as well to the two-time steps case C. A paper on the main results of the *4th international PIV Challenge* will be published at *Experiments in Fluids* in 2015 in which, based on ground truth data from DNS, direct comparisons will be made available of results for case D gained by STB and a subsequent innovative interpolation scheme named *FlowFit* (see next chapter) - which was necessary due to data requested on a regular grid - with those from recent advanced tomo PIV evaluation schemes which use as well temporal

information for the enhancements of the tomographic reconstruction quality (like MTE, Novara et al. 2010) *and* of the iterative 3D cross-correlation results (like FTC, Lynch and Scarano 2013).

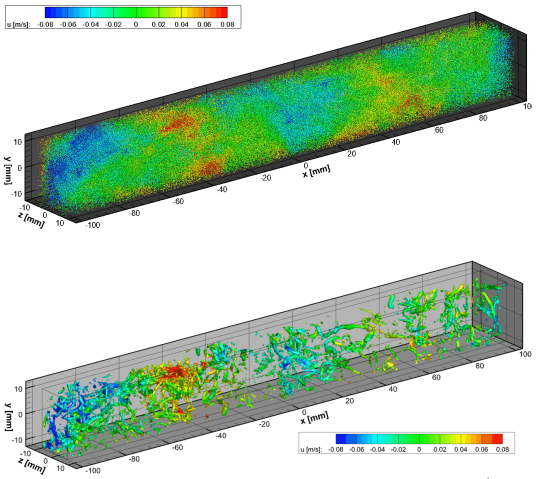

Figure 3: Overview of particles at one time step of 4th PIV Challenge Case D reconstructed with STB (top) and iso- - surfaces of 3D vorticity from FlowFit interpolation onto regular grid (bottom) both colour coded by u-velocity

FLOW-FIT INTERPOLATION SCHEME

After the STB evaluation has been finalized a novel interpolation scheme onto an Eulerian regular grid (named *FlowFit,* developed at DLR) has been applied on each time step of the estimated dense field of irregularly distributed velocity information given at each particle location within the ensemble of Lagrangian tracks. The interpolation scheme is based on an iterative optimization approach using quadratic B-splines in each of 3D cells, which are sized typically by a relative mean value between 0.05 and 0.25 ppc (particles per cell) and build up a regular high spatial resolution 3D array within the measurement volume. Each component of the flow field is modeled as a weighted sum of three-dimensional and evenly spaced quadratic B-splines. In order to evaluate this flow field on arbitrary coordinates, the weights have to be determined according to the known flow speeds at certain locations. This results in a linear equation system where for each known flow speed at some particular position three equations are created. In addition to these equations based on the measurements other equations are used to regularize the equation system by penalizing non-zero curvatures (which is known in combination with spline fitting as "smoothing spline") and optionally by penalizing non-zero divergencies (for incompressible flows) on a regular grid. This results in an overdetermined system where measurements and different kinds of regularizations can be weighted differently depending on how strong the smoothing effect should be, for example. In our current implementation, this equation system is solved iteratively via the conjugate-gradient algorithm. An obvious advantage of the briefly described interpolation method is that local values can be sampled on arbitrary grids and 3D vorticity and other values from the velocity gradient tensor can be calculated directly by derivatives of the respective B-spline.

EXAMPLES OF APPLICATION TO EXPERIMENTAL DATA

Two examples of application of the STB method to experimental tests in turbulent and transitional flows are shown in figures 4 and 5. In figure 4 a zoom into an instantaneous snapshot of the flow measured in the turbulent periodic hill water tunnel at TU Munich (ERCOFTAC test case 81) (see details at Rapp and Manhart 2009) and correspondent particle track information around one time instant represented as well by 3D-vorticity iso-contour surfaces (by FlowFit) are shown. The tracks are colour coded by spanwise Lagrangian acceleration showing extended regions of large values close to strong vortices, but as well small scale vortices, which are indicated by the arbitrary curvatures of many individual particle tracks in close proximity. More information on the experimental STB set-up and results showing as well global and local statistical approaches on the basis of a large amount of Lagrangian and Eulerian velocity and acceleration data is shown in Schröder et al. (2015).

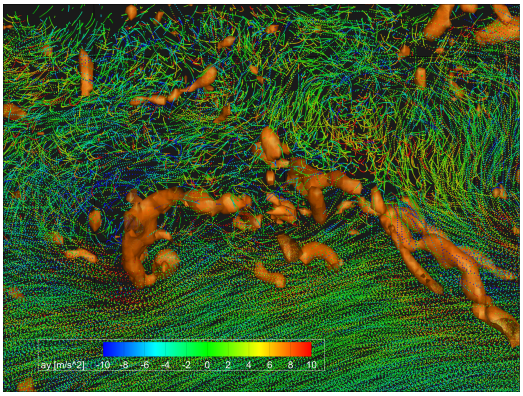

Figure 4: Detailed view of the measured flow in the turbulent periodic-hill water tunnel with colour coded spanwise Lagrangian acceleration derived from moving 3rd order polynomials of track length 15 and iso-surfaces of 3D-vorticity both from STB evaluation and FlowFit.

In figure 5 (top) the result of an STB evaluation over 500 time steps measuring the flow of a transitional jet in water at U = 0.5 m/s is shown. The jet has been observed with three high-speed cameras only with a relatively low spatial resolution at 1 kHz. The STB scheme tracked ~ 11.000 particles per time step on the basis of particle images with a density of ppp ~ 0.03. Following the track identification process moving 3rd order polynomials of length 19 have been applied to the found particle positions along all individual tracks.

Clearly the advantage of the present PTV method in relation to correlation based methods is visible by the shear independent measurement of single particle tracks,

enabling to follow even the entrainment of individual fluid elements. In figure 5 (bottom) the particles in the outside vicinity of the jets shear layer are forced to a spiralling motion due to pressure fluctuations caused by passing vortex rings, as shown in figure 6 (left). Thus the method can be applied as well to passive scalar dispersion and particle laden flow investigations.

Furthermore the overall shear layer and core-flow development can be visualized quantitatively without bias-errors and low-pass filtering effects. The same holds for the Reynolds stress tensor which can be estimated by an appropriate bin-averaging approach while the bin-shape and size can be adapted to symmetries in the flow, the mean velocity gradients and number of available independent samples in order to present converged turbulence statistics.

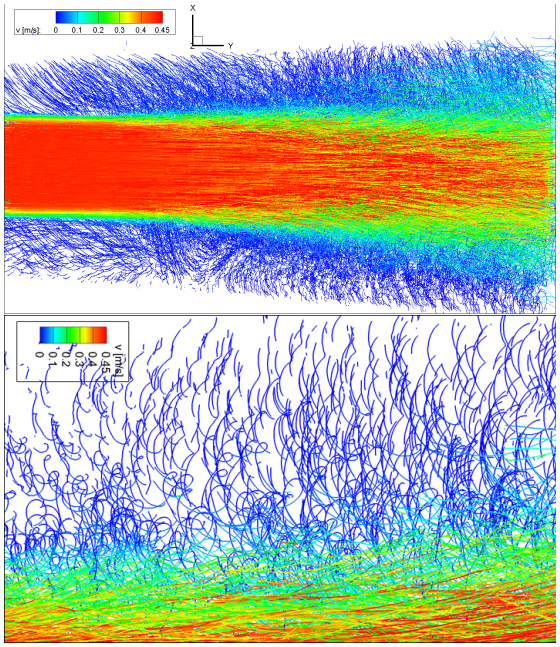

Figure 5: Middle-cut volume through a transitional jet flow showing all particle tracks reconstructed by STB over 500 time-steps. Corresponding time series of particle images have been acquired by three CMOS cameras only at 1 kHz (top). Tracks showing particles in the region outside the jet shear layer forced to a spiralling motion by the unsteady pressure fields of passing vortices (bottom)

In Fig. 6 (left) an instantaneous velocity volume of the transitional jet at U = 0.5 m/s core velocity is shown by 21 time-step tracks colour coded by the streamwise velocity, together with iso-surfaces of 3D vorticity of the middle step gained from a FlowFit interpolation. Clearly the thin shear vorticity is visible at the nozzle exit from which vortex rings develop due to Kelvin-Helmholtz instabilities. Further downstream secondary vortices evolve with streamwise orientation, leading to turbulent flow features and respective small scale fluid motion. In Figure 6 (right) iso-surfaces of the streamwise component of Lagrangian acceleration, calculated by FlowFit are color coded for the same time step. It is clearly visible that large accelerations (more than 10 m/s²) are present in the vicinity and inside of vortex rings and tubes. As vortices in incompressible flows are locations of low pressure values the Lagrangian accelerations around such strong vortices are pointing in average towards the vortex center. From integration of the Poisson equation along the given data field of material derivatives of the particle velocities (= Lagrangian acceleration) a time-resolved 3D pressure distribution can be calculated as outlined by Lui and Katz (2006) and Novara and Scarano (2013). As STB directly delivers the particle acceleration after temporal fitting in a high spatial resolution the relation and coupling of 3D pressure and velocity fields can be investigated for the first time in detail with experimental data, assuming the knowledge of the respective boundary conditions.

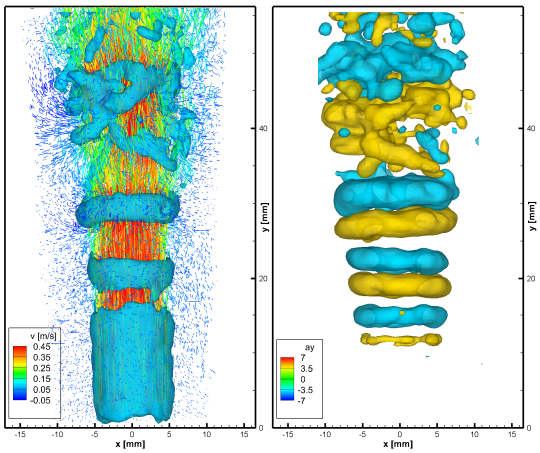

Figure 6: Middle-cut volume through a transitional jet showing 21 time steps particle tracks reconstructed by STB (c.c. by streamwise velocity) and iso-surfaces of vorticity (FlowFit) at the middle step (left). Iso-surfaces of streamwise acceleration at the same time-step gained by feeding particle accelerations into FlowFit (right)

CONCLUSIONS

The newly developed 4D-PTV measurement technique Shake-The-Box (STB) enables the investigation of spatial and temporal dynamics of coherent structures and Lagrangian particle tracks at high accuracies and relatively low computational costs. The technique allows studying the complexity of turbulent flows in much greater detail than before. Especially the possibility to achieve a very high spatial resolution for profiles of bin-averaged velocity components together with the full Reynolds stress tensor is of prominent interest for turbulence shear flow research. Taking additional advantages of using the combined data of Lagrangian and Eulerian reference frames for investigating the role of coherent structures and the corresponding dynamics of Lagrangian tracks for the turbulence production have just started.

REFERENCES

Adrian, R.J. (1997) Dynamic ranges of velocity and spatial resolution of particle image velocimetry, *Meas Sci Technol* 8(12)):1393

Atkinson, C. and Soria, J. (2009) An efficient simultaneous reconstruction technique for tomographic particle image velocimetry, *Exp. Fluids* 47, 563–578

Elsinga, G.E., Scarano, F., Wieneke, B. and Van Oudheusden, B.W. (2006) Tomographic particle image velocimetry, *Exp. Fluids*, Vol. 41, pp. 933-947.

Kähler, C.J., Scharnowski, S. and Cierpka, C. (2012) On the uncertainty of digital PIV and PTV near walls, *Exp Fluids* 52 (2012): 1641-1656

Liu, X. and Katz, J. (2006) Instantaneous pressure and material acceleration measurements using a four-exposure PIV system, *Exp Fluids,* 41: 227–240.

Lynch, K. and Scarano, F. (2013) A high-order time-accurate interrogation method for time-resolved PIV, *Meas. Sci. Technol.* 24 035305

Maas, H.G., Gruen, A. and Papantoniou, D. (1993) Particle Tracking velocimetry in three-dimensional flows Part I: Photogrammetric determination of particle coordinates, *Exp Fluids*, Vol. 15, pp. 133-146

Malik, N.A., Dracos, Th. and Papantoniou, D.A. (1993) Particle Tracking velocimetry in three-dimensional flows Part II: Particle tracking, *Exp Fluids*, Vol. 15, pp. 279-294

Novara, M., Batenburg, K.J., Scarano, F. (2010) Motion tracking-enhanced MART for tomographic PIV, *Meas. Sci. Technol.* 21 035401

Novara, M., and Scarano, F. (2013), A particle-tracking approach for accurate material derivative measurements with tomographic PIV, *Exp Fluids,* 54:1584.

Ouellette, N. T., Xu, H. and Bodenschatz, E. (2006), A quantitative study of three-dimensional Lagrangian particle tracking algorithms, *Exp. Fluids* 40, 301-313

Rapp, C. and Manhart, M.(2011), Flow over periodic hills: an experimental study, *Exp Fluids*, 51:247–269.

Scarano, F. (2013) Tomographic PIV: principles and practice. *Meas. Sci. Technol.* 24 012001, doi 10.1088/0957-0233/24/1/012001

Schanz, D., Gesemann, S., Schröder, A., Wieneke, B., Novara, M. (2013a) Non-uniform optical transfer functions in particle imaging: calibration and application to tomographic reconstruction*, Meas. Sci. Technol.* 24 024009

Schanz, D., Schröder, A., Gesemann, S., Michaelis, D., Wieneke, B. (2013b) 'Shake The Box': A highly efficient and accurate Tomographic Particle Tracking Velocimetry (TOMO-PTV) method using prediction of particle positions*, 10th Int. Symp. on PIV*, 01. - 03. July 2013, Delft, The Netherlands.

Schanz, D., Schröder, A., Gesemann, S. (2014), 'Shake The Box' - a 4D PTV algorithm: Accurate and ghostless reconstruction of Lagrangian tracks in densely seeded flows, *17th Int. Symp on Appl. Laser Techniques to Fluid Mechanics,* 07. – 10. July 2014, Lisbon, Portugal

Schröder, A., Schanz, D., Geisler, R., Willert, C. and Michaelis, D. (2013), Dual-Volume and Four-Pulse Tomo PIV using polarized laser lights, *10th Int. Symp. on PIV*, July 1-3., Delft, The Netherlands.

Schröder, A., Schanz, D., Michaelis, D., Cierpka, C., Scharnowski, S., Kähler, C.J. (2015) Advances of PIV and 4D-PTV "Shake-The-Box" for turbulent flow analysis – the flow over periodic hills, accepted for publication at *Flow, Turbulence and Combustion*, Springer

Wieneke, B. (2007) Volume self-calibration for Stereo PIV and Tomographic PIV, *Exp. Fluids* 45, 549-556

Wieneke, B. (2013) Iterative reconstruction of volumetric particle distribution, *Meas. Sci. Technol.* 24, 024008

Table 1: Comparison of tomographic reconstruction (MLOS-SMART) and subsequent particle peak identification to tracking results of STB for a synthetic particle image data-set at a converged time step

ppp	0.125	0.1	0.075	0.05	0.025	0.01
Real particles	110868	88584	66439	44233	22060	8904
Undetected particles, SMART [%]	9387 (8.48 %)	3400 (3.83 %)	1119 (1.68 %)	405 (0.91 %)	135 (0.61 %)	47 (0.53 %)
Undetected particles, STB [%]	483 (0.43 %)	268 (0.30 %)	104 (0.16 %)	63 (0.14 %)	18 (0.06 %)	9 (0.10 %)
Ghost particles, SMART	282090 (254.8 %)	206990 (233.7 %)	121680 (183.1 %)	42229 (95.5%)	3721 (16.8 %)	134 (1.5%)
Ghost particles, STB	36.5 (0.033 %)	16.1 (0.018 %)	5.8 (0.008 %)	3.5 (0.008 %)	1 (0.005 %)	0 (0.0 %)
Avg. position error, SMART [px]	0.308	0.278	0.243	0.201	0.155	0.135
Avg. position error, STB [px]	0.0177	0.0076	0.0023	0.0008	0.0005	0.0002